THE JOURNAL OF PHYSICAL CHEMISTRY A

Article

pubs.acs.org/JPCA

Computational Vibrational Spectroscopy of HDO in Osmolyte−Water Solutions

Hochan Lee,[†,‡,∥] Jun-Ho Choi,[†,‡,∥] Pramod Kumar Verma,[†,‡] and Minhaeng Cho*[,†,‡]

[†]Center for Molecular Spectroscopy and Dynamics, Institute for Basic Science and [‡]Department of Chemistry, Korea University, Seoul 02841, Republic of Korea

Supporting Information

ABSTRACT: The IR absorption and time-resolved IR spectroscopy of the OD stretch mode of HDO in water was successfully used to study osmolyte effects on water H-bonding network. Protecting osmolytes such as sorbitol and trimethylglycine (TMG) make the vibrational OD stretch band red-shifted, whereas urea affects the OD band marginally. Furthermore, we recently showed that, even though sorbitol and TMG cause a slow-down of HDO rotation in their aqueous solutions, urea does not induce any change in the rotational relaxation of HDO in aqueous urea solutions even at high concentrations. To clarify the underlying osmolyte effects on water H-bonding structure and dynamics, we performed molecular dynamics (MD) simulations of a variety of aqueous osmolyte solutions. Using the vibrational solvatochromism model for the OD stretch mode and taking into account the vibrational non-Condon and polarization effects on the OD transition dipole moment, we then calculated the IR absorption spectra and rotational anisotropy decay of the OD stretch mode of HDO for the sake of direct comparisons with our experimental results. The simulation results on the OD stretch IR absorption spectra and the rotational relaxation rate of HDO in osmolyte solutions are found to be in quantitative agreement with experimental data, which confirms the validity of the MD simulation and vibrational solvatochromism approaches. As a result, it becomes clear that the protecting osmolytes like sorbitol and TMG significantly modulate water H-bonding network structure, while urea perturbs water structure little. We anticipate that the computational approach discussed here will serve as an interpretive method with atomic-level chemical accuracy of current linear and nonlinear time-resolved IR spectroscopy of structure and dynamics of water near the surfaces of membranes and proteins under crowded environments.

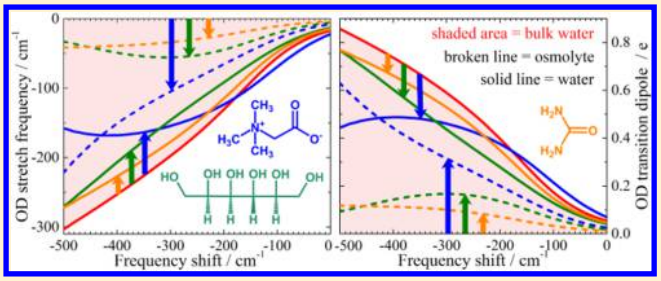

I. INTRODUCTION

Osmolytes are small organic molecules that are ubiquitously used by almost all living beings to respond to cellular stress such as potentially harmful fluctuations in temperature, pressure, solution composition, etc.[1] The mammalian kidney is one such viscera under osmotic stress, where osmolytes such as glycerophosphocholine, sorbitol, and trimethylglycine (TMG) are often accumulated to counteract the deleterious effects of the high renal urea (destabilizing osmolyte) and salt concentrations.[1−3] Thus, their effects on water H-bonding network structure has long been an important subject of study.[4−6]

The networking structure of intermolecular water H-bond is continuously changing on extremely fast time scale, and hence the characterization of the network dynamics inevitably requires ultrafast spectroscopic methods that are sensitive to both the time evolution of the water H-bond number and strength.[7−17] The frequency of the OD stretching vibration of HDO molecule is very sensitive to its H-bonding interactions with surrounding water molecules.[18] Therefore, it has been routinely used to investigate the water H-bonding dynamics in not just bulk water[13,14,19−22] but also other solutions containing salts,[23−26] water-miscible organic solvent molecules,[27,28] and osmolytes.[29−32] More precisely, the HDO has the capability to form multiple H-bonds with surrounding water molecules as well as other dissolved species (osmolyte, amphiphile, salt, etc). Consequently, its vibrational dynamics provides important information from HDO's point of view on H-bond making and breaking processes and solvation dynamics. However, the information being provided by the OD probe is strictly from the water's point of view and does not provide any information on how a given osmolyte dictates water's choice to be H-bonded either with another water or a third molecular component (e.g., protein or solute) in solution. Therefore, to have a stereoscopic and complementary view on osmolyte-induced changes in water structure, we recently employed two different IR probes that are the OD stretch mode of HDO and the azide asymmetric stretching vibration of hydrazoic acid.[31] In addition, we performed molecular dynamics (MD) simulations and graph theory analyses to study both the local (reflecting just the fleeting environment around individual water molecules) and global (spatially large-scale structures of water H-bonding network and osmolyte aggregate) changes in the

Received: June 22, 2016
Published: June 24, 2016

DOI: 10.1021/acs.jpca.6b06305
J. Phys. Chem. A 2016, 120, 5874−5886

water structure.[33] Altogether, we found that solute−water partnership and H-bond strength are crucially dependent on the type and concentration of osmolytes. The protecting osmolytes, for example, sorbitol and TMG, were found to form extended large-scale networklike aggregates causing significant disruption of water H-bonding network structure in concentrated osmolyte solutions. Conversely, urea neither weakens nor strengthens the H-bonding network of water, does not affect the solute-water partnership, fits into water's tetrahedral H-bonding structure, and tends to form localized clusterlike aggregates in highly concentrated urea solutions. Related to such vibrational spectroscopic experiments, it is important to test the predictions of current simulation models against these experimental results.

In this paper, we focus on the theoretical vibrational spectroscopy of aqueous (isotopically diluted water containing a small amount of HDO to avoid coupling between OD groups) solutions of sorbitol, TMG, and urea, at various concentrations. Our study builds on the earlier work of ours as well as others.[33−35] Recently, our group developed a distributed vibrational solvatochromism model[36] to numerically calculate the linear and nonlinear vibrational spectra of the amide I mode of peptide system[37−40] as well as of IR probes such as nitrile (−CN),[41,42] thiocyanato (−SCN),[41,42] azido ($-N_3$),[43] and carbon monoxide (CO)[44] attached to biomolecules. Although the transition dipole moments of these incorporated IR probes were found to be comparatively insensitive to local electrostatic environment, that of the HDO is strongly dependent on the local H-bond configuration.[45] This vibrational solvatochromism model was further improved by considering non-Condon effect on the vibrational transition dipole moment of water molecule.[34,46−51] This extended approach was used to numerically simulate IR absorption and Raman scattering of OD stretch mode of HDO in highly concentrated solution of sodium chloride (NaCl) and potassium thiocyanate (KSCN).[34] Our approach of using the solvatochromic charge model to describe the transition dipole vector considers not only the *z*-component pointing toward the OD bond axis (see Scheme 1)

Scheme 1. Molecular Structure of the Renal Osmolytes Studied in the Present Work

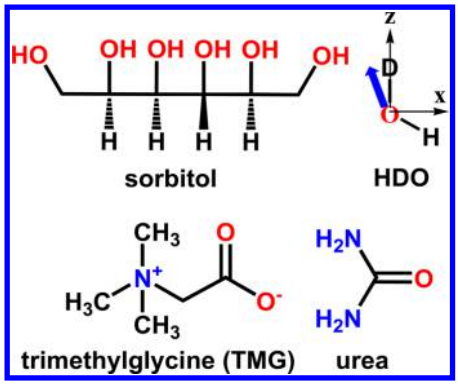

but also the *x*-component of the transition dipole moment of HDO, which was ignored by most of the other research groups.[52−54] In ref 34, the *x*-component of the OD transition dipole moment was found to be important in understanding the asymmetric line shape of the OD IR absorption spectrum in highly concentrated salt solutions. Herein, the improved solvatochromism model with inclusion of non-Condon effect on HDO vibrational transition dipole moment is used to obtain fluctuating vibrational frequencies and vibrational transition dipole vector followed by numerical simulation of the IR spectra in aqueous solutions of protecting osmolytes (sorbitol and TMG) and urea (destabilizing osmolyte), at various concentrations. Using both our vibrational solvatochromism theory and MD simulation method, we here investigate the osmolyte effects on the OD stretch mode frequency as well as on the rotational relaxation rate of HDO in aqueous osmolyte solutions.

The organization of this paper is as follows. In Section II, we briefly describe the theory of the vibrational solvatochromism while explaining the relationship between the vibrational frequency and the transition dipole moment with electrostatic potential at atomic sites positioned within a given HDO in aqueous osmolyte solutions. In Section III, we present the distributions of the OD stretch mode vibrational frequency and the *x*- and *z*-components of the transition dipole vector of HDO for all the three aqueous osmolyte solutions at various concentrations. In Section IV, the numerically simulated IR absorption spectra of HDO and the rotational anisotropy of OD group in osmolyte solutions are directly compared to the experimentally measured results; and in Section V, the main results are summarized with a few concluding remarks.

II. VIBRATIONAL SOLVATOCHROMISM MODEL

An improved vibrational solvatochromic charge model was used to obtain the fluctuating transition dipole vector of OH stretch mode of H_2O and to numerically calculate the IR absorption and Raman scattering spectra of the symmetric and asymmetric OH stretch modes of H_2O in water.[48] The charge-response kernel approach[36] was employed to calculate the transition dipole moments of polarizable water molecules. The resultant IR and Raman scattering spectra of the water OH stretch mode were found to be in quantitative agreement with the experimentally obtained vibrational spectra of liquid water.[48] We also developed a vibrational solvatochromism model for the OD stretch mode of HDO to calculate the vibrational frequency and transition dipole moment of HDO in pure liquid water.[34] This vibrational solvatochromism model was further used to numerically simulate the IR absorption and Raman scattering spectra of the OD mode in pure water as well as in salt solutions. The procedure for the calculation of the vibrational spectrum of the OD stretch mode in liquid water used in the present work is briefly described below.

First, the relationship between the instantaneous OD vibrational frequency and the electrostatic potential created by the surrounding water molecules or osmolyte molecules or both around OD group was established as[36]

$$\Delta\omega(\phi) = \omega(\phi) - \omega_0 = \sum_{m=1}^{n} l_m \phi(\mathbf{R}_m) \quad (1)$$

where l_m and ϕ ($\mathbf{R}_m$) correspond the vibrational solvatochromic charge of the *m*th interaction site of an isotope-substituted water HDO and the electric potential at the position $\mathbf{R}_m$ of the *m*th site, respectively. The reference frequency ω_0 is 2812.5 cm^{-1}, which is the quantum chemistry calculation result for an isolated HDO molecule. The three interaction sites are located at O atom (site 1), D atom (site 2), and H atom (site 3) in an HDO molecule. The vibrational solvatochromic charges are l_O = −0.022 013 *e*, l_D = 0.028 628 *e*, and l_H = −0.006 6150 *e* that were calculated by performing extensive QM calculations and the multivariate least-squares analyses of a number of HDO-

DOI: 10.1021/acs.jpca.6b06305
J. Phys. Chem. A 2016, 120, 5874−5886

Table 1. Concentration and Number of Molecules of Osmolytes Employed in the Simulation

	concentration M (m)	number of molecule		concentration M (m)	number of molecule
TMG	1.09 (1.17)	21	sorbitol	4.08 (7.99)	144
TMG	2.10 (2.50)	45	sorbitol	4.98 (12.71)	229
TMG	3.28 (4.44)	80	urea	1.03 (1.05)	19
TMG	5.04 (8.55)	154	urea	3.11 (3.44)	62
sorbitol	1.00 (1.11)	20	urea	5.08 (6.16)	111
sorbitol	2.04 (2.66)	48	urea	7.11 (9.66)	174
sorbitol	3.07 (4.83)	87			

$(H_2O)_n$ clusters using eq 1.[34] The imposed condition of $(\sum_{m=1}^{3} l_m = 0)$, which is based on the assumption that there is no intermolecular charge transfer, ensures that a uniform electrostatic potential makes no frequency shift. Afterward, the values of vibrational solvatochromic charges obtained from eq 1 were used to calculate OD stretch mode frequency in aqueous solutions of urea, sorbitol, and TMG. The electric potentials at the interaction sites were calculated[55] using charges from electrostatic potentials using a grid-based method partial charges of solvent H_2O and osmolyte molecules, which were obtained from the corresponding density functional theory calculations.[56]

In principle, as shown in ref 36, the contributions from the distributed vibrational solvatochromic dipoles and higher multipoles can be neglected as long as the number of interaction sites with properly determined vibrational solvatochromic charges is sufficiently many. As shown in our previous studies on the vibrational solvatochromic processes of the O−H stretch modes of water and the O−D stretch mode of HDO in water, the three interaction site model with accurately calculated vibrational solvatochromic charges works quantitatively well for describing solute−solvent electrostatic interaction-induced frequency shifts.[34,48] Hence, the term taking into consideration the charge−potential interaction, eq 1, is sufficiently accurate and useful in describing the solvatochromic frequency shift of O−D stretch mode of HDO in various aqueous solutions. In fact, the present theoretical approach developed by us differs from the earlier studies that provided numerically simulated vibration spectra such as IR absorption,[49,50,52,53] Raman scattering,[50,53] and two-dimensional IR spectra[49] of the O−D (O−H) stretch mode of HDO in H_2O (D_2O). They employed an empirical parameter map on the relationships between both local solvent electric field and electric field gradient and the OD (OH) frequency and between them and transition dipole moment in liquid water. Here, we used our distributed interaction site model with three sites of H, D, and O atoms, since this model is chemically accurate for simulating IR absorption spectra of HDO in not just water but also high salt solutions.[34,48]

As mentioned earlier, the OD vibrational transition dipole moment is strongly dependent on the configuration of the surrounding water molecules, which is known as vibrational non-Condon effect.[34,52,53] It was shown that the OD vibrational transition dipole vector that needs careful treatment considering the polarizable nature of a water molecule can be expressed by employing a distributed interaction site model of vibrational solvatochromism (details in ref 36).

$$\left(\frac{\partial \boldsymbol{\mu}(\phi)}{\partial Q_\alpha}\right)_{\mathrm{eq}} \approx \left(\frac{\partial \boldsymbol{\mu}_0}{\partial Q_\alpha}\right)_0 + \sum_{m=1}^{N}\sum_{n=1}^{N} \tilde{K}_{mn}\mathbf{R}_m\phi(\mathbf{R}_n) + \sum_{m=1}^{N} \mathbf{m}_m\phi(\mathbf{R}_m) \quad (2)$$

The term $\boldsymbol{\mu}(\phi)$ represents the ground-state dipole moment of the solute depending on the solvent electric potential. $(\partial\boldsymbol{\mu}(\phi)/\partial Q_\alpha)_{\mathrm{eq}}$ is the derivative of $\boldsymbol{\mu}(\phi)$ with respect to Q_α at the HDO equilibrium geometry in the presence of ϕ, where Q_α is the αth normal coordinate of the solute. The charge response kernel (CRK) $\tilde{K}_{mn}$ is defined within the site representation of the nonlocal polarizability density as follows

$$\tilde{K}_{mn}(\mathbf{Q}_0) \equiv \sum_{\mathrm{e}\neq\mathrm{g}} \frac{c_{\mathrm{ge}}^{m}(\mathbf{Q}_0)c_{\mathrm{eg}}^{n}(\mathbf{Q}_0)}{E_{\mathrm{g}}^{0}(\mathbf{Q}_0) - E_{\mathrm{e}}^{0}(\mathbf{Q}_0)} \quad (3)$$

where $c_{\mathrm{ge}}^{\mathrm{m}}(\mathbf{Q}_0)$ indicates the g ↔ e transition charge at the site m. The CRK, $\tilde{K}_{mn}(\mathbf{Q}_0)$, is basically a second-rank tensor (3 × 3 matrix) in the site representation, which is related to the molecular polarizability of the electronic ground state. $(\partial\boldsymbol{\mu}_0/\partial Q_\alpha)_0$ in eq 2 is the OD stretch transition dipole of an isolated HDO molecule, and $\mathbf{m}_m$ associated with the site m is a vector in the Cartesian coordinate frame of the HDO molecule. The second term on the right-hand side of eq 2 originates from the induced dipole moment in the presence of local electric potential, whereas the third term originates from the solvation-induced structural distortion of the solute molecule. This theoretical approach has been successfully applied to numerically simulate the OH stretch bands of H_2O in liquid water[48] as well as the OD stretch band of HDO in liquid water[34] and aqueous salt solutions.[34]

Both the CRK matrix elements $\{\tilde{K}_{mn}\}$ and the vector elements $\{\mathbf{m}_m\}$ obtained using the multivariate least-square analysis method (eq 2) have been reported earlier in detail in ref 34. Applying the symmetry restraint to the CRK matrix, the values of the six independent CRK elements, K_{11}, K_{12}, K_{13}, K_{22}, K_{23}, and K_{33}, were found to be 0.000 192 63, −0.000 202 98, −0.000 004 2389, 0.000 322 07, −0.000 111 34, and 0.000 123 18 e^2/Å cm^{-1}, respectively. The six vector elements $[m_1]_x$, $[m_2]_x$, $[m_3]_x$, $[m_1]_z$, $[m_2]_z$, and $[m_3]_z$ were also calculated with values 0.000 004 9958, 0.000 110 24, −0.000 115 24, 0.000 273 84, −0.000 414 25, and 0.000 140 41 e^2/cm^{-1}, respectively. Among all the CRK matrix elements, the K_{22} associated with the D atom is much larger than the other diagonal elements of K_{11} (for the O atom site) and K_{33} (for the H atom site). Similarly, among all the vector elements $\{\mathbf{m}_m\}$, $[m_2]_z$ is the largest, because the z-component of the OD stretching vibration contributes mostly to the OD transition dipole moment. In addition, the z-component of $(\partial\boldsymbol{\mu}_0/\partial Q_\alpha)_0$ is the largest value of 0.193 e, while the x- and y-components have values of −0.041 and 0.00 e, respectively.[34] Since the fluctuation amplitude of the y-component is negligible, we ignored the contribution from the y-component in determining the OD transition dipole vector magnitude hereafter. The magnitude of the transition dipole moment of the OD stretch mode of HDO is estimated to be 0.0195 in unit of $e{\cdot}a_0$, where the vibrational amplitude is 0.0987a_0. With these predetermined values and eq

DOI: 10.1021/acs.jpca.6b06305
J. Phys. Chem. A 2016, 120, 5874−5886

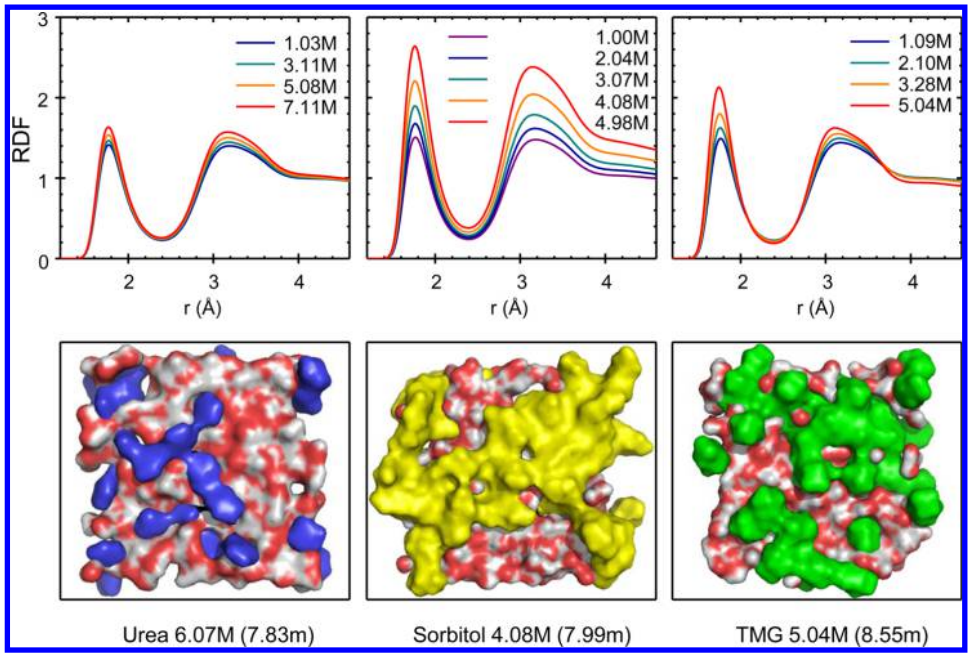

Figure 1. (upper) RDFs between water oxygen and water hydrogen atoms. (lower) Snapshot structures of the osmolyte−osmolyte aggregates and water H-bonding networks in aqueous solutions of urea (blue), sorbitol (yellow), and TMG (green).

2, we could calculate both the *x*- and *z*-components of the OD vibrational transition dipole vector of a given HDO molecule. The OD transition dipole vector makes an angle of ∼12° with the OD bond axis as shown in Scheme 1 (see the blue arrow on HDO). Our concern is to emphasize the contribution of the *x*-component of the OD transition dipole vector that is not to be ignored, because its contribution significantly increases as the concentrations of ionic species in highly concentrated salt solutions increase.[34]

III. OD STRETCH MODE FREQUENCY AND TRANSITION DIPOLE MOMENT IN OSMOLYTE SOLUTIONS

A. Molecular Dynamics Simulation Method. The osmolyte concentrations along with the corresponding numbers of the three different osmolyte molecules in a given MD simulation box containing 1000 TIP3P water molecules are arranged in Table 1. The highest concentrations of the three different osmolytes studied in this work are close to their solubility limits. Osmolyte molecules were described[57] using General Amber Force Field parameters, and the corresponding restrained electrostatic potential[58] charges were taken from our previous MD simulation work.[33] The cutoff distance for the nonbonding interaction was assumed to be 10 Å, and the particle mesh Ewald method[59,60] was used for considering the long-range electrostatic interactions. The water−osmolyte binary mixture was first energy-minimized with the steepest descent method followed by the conjugate gradient method, and subsequently, the equilibrium MD simulations were run. A constant *N*, *p*, and *T* ensemble simulation at $p = 1$ atm and $T = 298$ K was performed for 10 ns to adjust the density of the binary system. An additional 10 ns at constant *N*, *V*, and *T* simulation at 298 K was also performed to reach its thermal equilibrium state. Finally, a 10 ns production run was performed at constant *N*, *V*, and *T* condition, where the simulation time step was 1 fs for MD trajectories, and atomic coordinates were saved every 5 fs for the subsequent statistical analysis and the numerical simulations of the OD stretch IR absorption and the rotational anisotropy in aqueous osmolyte solutions.

B. Osmolyte Aggregate and Water H-Bonding Network Structures. Our recent experimental and theoretical works on osmolyte−water binary system have provided new insights into both the local and global changes in the water H-bond network as well as on the osmolyte−osmolyte aggregation behavior.[31,33] Let us briefly discuss the water−water radial distribution function (RDF) between water oxygen and water hydrogen (O_w−H_w) in three different osmolytes at various concentrations (see Figure 1). At low concentrations (∼1 M), the O_w−H_w RDFs are similar to that of pure liquid water, which suggests no significant disruption of water H-bonding network structures. As the concentration increases, both the first and the second peaks of the O_w−H_w RDF rise significantly in the case of sorbitol, which indicates a long-range impact on water structure by sorbitol. Addition of TMG increases mostly the first peak height of the O_w−H_w RDF suggesting perturbation to the water structure only in the immediate vicinity of TMG. Urea, at all concentrations, does not bring any significant changes to the water H-bonding network structures. In Figure 1, we present some representative snapshot structures of the aqueous solutions of urea, sorbitol, and TMG depicting the global changes in the water H-bond network. Although the concentrations of the three osmolytes are nearly similar (∼8 m), the aggregation tendency of urea (blue color species, localized cluster) is markedly different from those of sorbitol (yellow color species) and TMG (green color species). The protecting osmolytes (sorbitol and TMG) adopt to a networklike aggregate structure in their highly concentrated aqueous solutions that is morphologically similar to that of the extended water H-bond network. Conversely, urea (destabilizing osmolyte) molecules fit into water's tetrahedral H-bonding structure and tends to form separated clusterlike aggregates at high concentrations. These quantitative differences in the morphological structures of osmolyte aggregates

DOI: 10.1021/acs.jpca.6b06305
J. Phys. Chem. A 2016, 120, 5874−5886

were noticed and emphasized with our spectral graph analysis method[33] that is a theoretical tool to probe the global changes in various composite systems.[61−65] In fact, these morphological differences between the protecting and destabilizing osmolytes are reflected in the experimentally measured data of the vibrational stretch mode and reorientation dynamics of HDO that provide information on the local water H-bonding network.

C. Distributions of OD Stretch Mode Frequency and Transition Dipole Moment. The distributions of the OD stretch mode frequency and transition dipole moment were obtained with 2 000 000 snapshot configurations taken from the MD trajectory for each osmolyte solution. First, a water molecule was randomly selected from the 1000 water molecules and then was replaced with HDO for subsequent calculations. We used eqs 1 and (2) to calculate the frequency and transition dipole moment of the OD stretch mode. To obtain statistically reliable ensemble average vibrational properties, for a single snapshot structure taken from MD trajectories, we repeated the above calculations 100 times by randomly choosing one water molecule at a time. Thus, the OD frequency and transition dipole moments were calculated for 200 million cases, and their distributions for three different osmolytes are plotted in Figure 2. With increasing concentration of the protecting osmolyte,

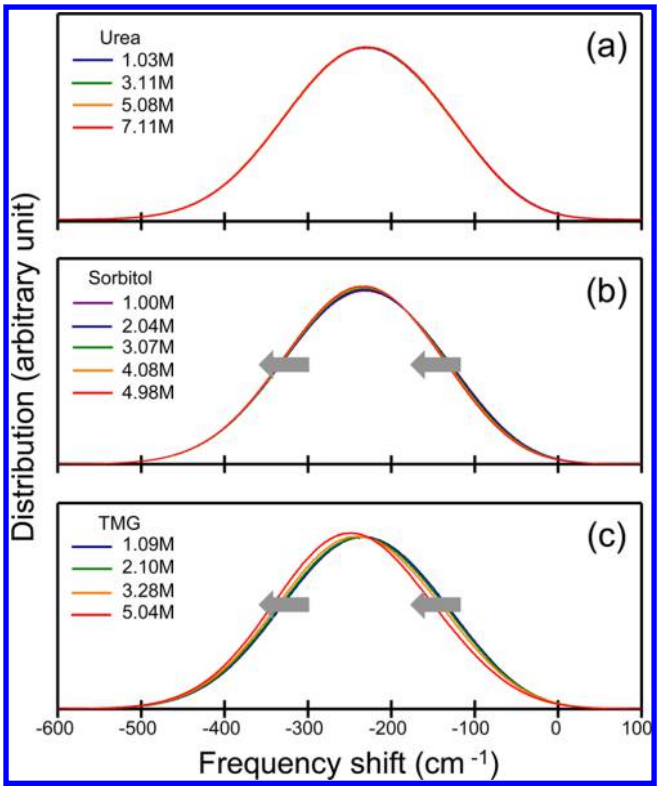

Figure 2. Frequency distributions of the OD stretch modes in the aqueous solutions of urea (a), sorbitol (b), and TMG (c) at various concentrations. The gray-colored arrow represents the red shift in the frequency distribution peak.

the OD frequency distribution shows a red shift. The magnitude of the frequency shift with respect to the bulk water is different for sorbitol and TMG. Addition of TMG causes a relatively large frequency shift compared to that of sorbitol. In contrast, addition of urea results in no significant change in the OD frequency distribution. A further insight is gained by looking into the distributions of the x- and z-components of the transition dipole vector of HDO in the three different osmolyte solutions as shown in Figure 3. Neither

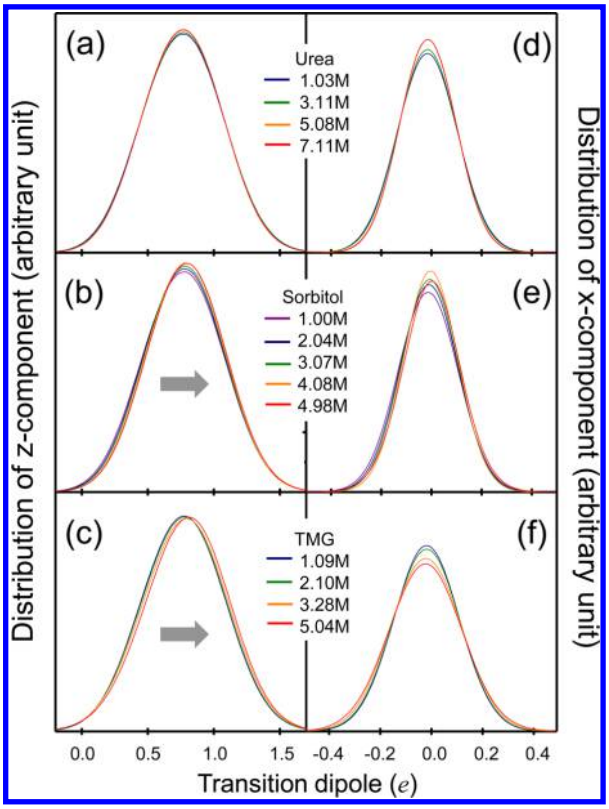

Figure 3. Distribution of the z-component (in e) of the OD transition dipole moment in urea (a), sorbitol (b), and TMG (c) solutions. Distribution of the x-component (in e) of OD transition dipole moment in urea (d), sorbitol (e), and TMG (f) solutions. The z-component distributions of the transition dipole moments of OD stretch in sorbitol and TMG solutions shift toward higher value as their concentrations increase.

x- nor z-component of the transition dipole vector of HDO shows any appreciable change with increasing concentration of urea, whereas the average magnitude of μ_z increases marginally with addition of the protecting osmolytes (sorbitol and TMG).

Now, let us examine the OD frequency shift (Figure 4) obtained from the average over the distributions (in Figure 2) and the magnitude of the transition dipole moment, $\sqrt{(\mu_x^2 + \mu_z^2)}$, with respect to the osmolyte concentrations. The red shift of the OD frequency in the presence of the protecting osmolytes (Figure 4a) is in good agreement with experimentally measured OD peak shifts. The absolute magnitudes of $|\vec{\mu}|$ exhibit an increasing tendency with the increasing concentration of the protecting osmolytes, but there is no concentration-dependent change of either the OD frequency or the $|\vec{\mu}|$ in the case of urea. Interestingly, the ratio $\langle|\mu_x|/|\vec{\mu}|\rangle$, which is the relative magnitude of the x-component of the transition dipole moment, does not change much with concentration for any of the three osmolytes. The ratio $\langle|\mu_x|/|\vec{\mu}|\rangle$ is 0.14−0.13, 0.15−0.16, and 0.14−0.13 for sorbitol (∼1−5 M), TMG (∼1−5 M), and urea (∼1−7 M), respectively. Although the x-component of the transition dipole vector is not the major factor, still it needs to be considered

DOI: 10.1021/acs.jpca.6b06305
J. Phys. Chem. A 2016, 120, 5874−5886

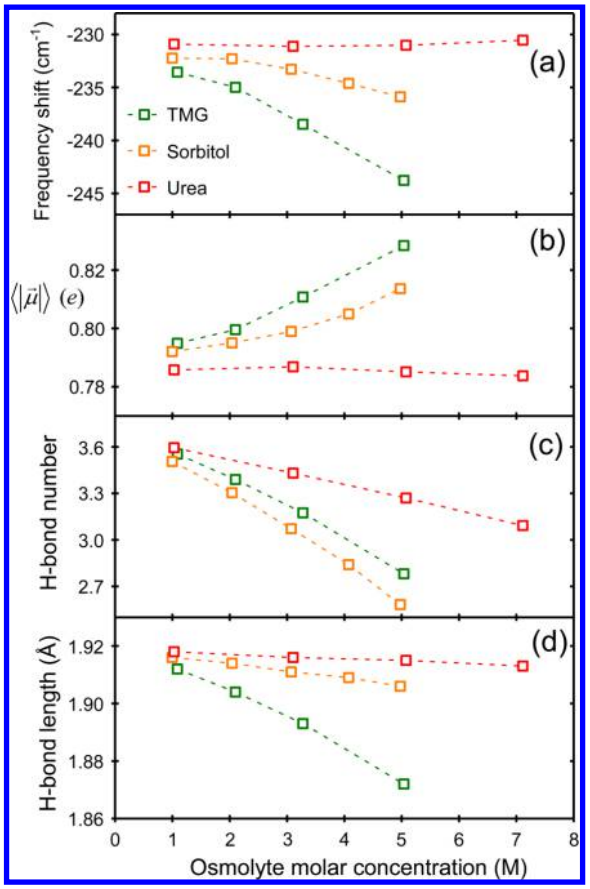

Figure 4. Ensemble averaged vibrational frequency shifts (in cm^{-1}) of the OD stretch mode as a function of various osmolytes concentrations (a). Concentration dependence of the transition dipole moment distributions of $|\vec{\mu}|$ (in e) (b), average H-bond number (c), and average H-bond length of a water (d) for aqueous solutions of sorbitol, TMG, and urea.

because it reflects the polarizable nature of water molecule and quantitatively contributes to the IR absorption line shape (vide infra).

To quantify the changes to the water H-bonding structure in the presence of osmolyte at different concentrations, the ensemble averaged H-bond number of a water molecule and the H-bond length between a pair of H-bonded water molecules were calculated. The distance criterion of an H-bond between water molecules was set to 2.41 Å.[34] The addition of osmolytes makes the H-bond number decrease (Figure 4c), but the extent of decrease varies according to the type of the osmolyte. Both sorbitol and TMG cause a large decrease in the H-bond number, which is in contrast with urea. TMG brings down the average H-bond length substantially, whereas sorbitol and urea cause a marginal drop in the H-bond length, suggesting water molecules near TMG are tightly packed. The concentration-independent behavior of urea toward the OD frequency shift, $|\vec{\mu}|$, and the H-bond length (Figure 4) agrees well with the notion that urea affects water H-bonding network structure very little both locally and globally.[33,35,66,67]

IV. COMPARISONS BETWEEN SIMULATED AND EXPERIMENTALLY MEASURED VIBRATIONAL SPECTRA

Although the MD simulations and graph spectral analyses have provided new insights into the osmolyte−osmolyte aggregate and water H-bonding network structures in aqueous osmolyte solutions, thus obtained results depend on set of used forcefield parameters in MD simulations.[68−70] Therefore, to confirm the validity of employed MD simulation method, the numerically simulated vibrational spectra obtained by combining an MD simulation method and the vibrational solvatochromism model without any adjustable parameters are directly compared to the ones obtained from the experiments on the isotopically diluted water in three different osmolytes at various concentrations. This is, in fact, one of the principal goals of the present work.

IV.A. Numerically Simulated O−D Infrared Absorption Spectra in Aqueous Osmolyte Solutions. Employing the MD simulation trajectories and theoretical solvatochromism models for the vibrational frequency and transition dipole moment of HDO (Section II), IR absorption spectra of the OD stretch mode was calculated in aqueous osmolyte solutions using following expression[71,72]

$$I_{\mathrm{IR}}(\omega) = \int_0^\infty \mathrm{d}t \mathrm{e}^{-i\omega t}\langle \mu(0)\mu(t)\exp[i\int_0^t (\omega(\tau) - \langle\omega_{10}\rangle)\mathrm{d}\tau]\rangle \mathrm{e}^{-t/2T_1} \quad (4)$$

where $\mu(t)$ is the vibrational transition dipole moment of the OD stretch mode of HDO. The exponential function inside the angular bracket on the right-hand side of eq 4 describes the vibrational dephasing process resulting from fluctuating vibrational transition frequency due to the interactions of the HDO with the surrounding water and the osmolyte molecules. As shown by the Skinner group, the transition dipole moment of OD stretch mode exhibits a high sensitivity to its local electrostatic environment.[52,53] That is to say, the H-bonding interaction with neighboring water molecules causes a dramatic increase of the OD transition dipole moment. The fluctuation of the transition dipole moment, $\mu(t)$ in eq 4, originates from the rotational motion of HDO and the non-Condon effect that are well-described by eq 2. The term $\omega_{10}(t) - \langle\omega_{10}\rangle$ describes the fluctuating part of the OD vibrational frequency, where $\langle\omega_{10}\rangle$ represents the ensemble average of $\omega_{10}(t)$ calculated by considering 200 million configurations. The multiplied exponential function, $\exp(-t/2T_1)$, is used for an ad hoc description of the vibrational population relaxation, where the lifetime of the vibrational excited state of the OD stretch mode, denoted as T_1, is known to be 1.45 ps.[73] Our recent experimental data revealed that the vibrational population lifetime of the OD stretch band is marginally dependent on the type and concentration of osmolytes.[31] Moreover, because the vibrational lifetime broadening is negligible in comparison to the effects from the distributions of the O−D frequencies as well as the O−D stretch transition dipole moments due to heterogeneous electrostatic environment, the IR absorption spectrum of the OD stretch mode depends mostly on the contributions from the inhomogeneous broadening as well as varying transition dipole moment due to non-Condon effect, rather than the vibrational lifetime.

The numerically simulated vibrational spectra of the OD stretch mode of HDO in three different osmolyte solutions are presented in Figure 5 along with the experimentally measured ones. Both the numerically simulated and the experimentally measured vibrational spectra agree with the observation of the

DOI: 10.1021/acs.jpca.6b06305
J. Phys. Chem. A 2016, 120, 5874−5886

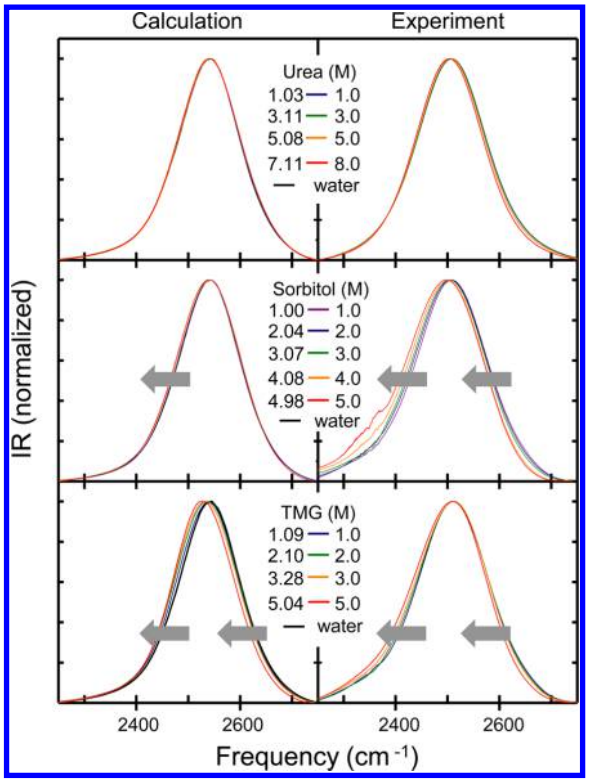

Figure 5. Numerically simulated IR spectra (left column) of the OD stretch mode of HDO in osmolyte solutions are directly compared with our experimentally measured spectra (right column). The gray-colored arrow indicates the red shift in the OD peak frequency with increasing concentration of osmolytes.

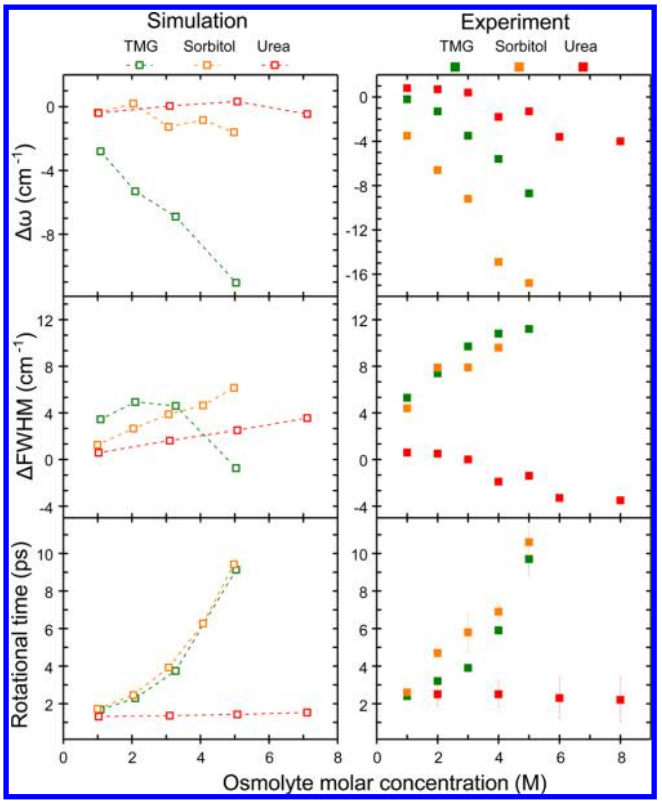

Figure 6. Peak frequency shift ($\Delta\omega = \omega_{\text{osmolyte-water}} - \omega_{\text{water}}$), the Δfwhm (= $\text{fwhm}_{\text{osmolyte-water}} - \text{fwhm}_{\text{water}}$), and the rotational time constants obtained from the numerically simulated results (left column) as a function of osmolyte concentrations are compared with the ones obtained from experimentally measured results (right column). The peak frequency shift and fwhm were determined by using pseudo-Voigt fits, and τ_{rot} was calculated using a mono-exponential ($r(t) = A\exp(-t/\tau_{\text{rot}}) + B$) function. The error bars are shown for the experimentally measured τ_{rot}.

red shift of the OD stretch band on addition of sorbitol and TMG. In the case of urea, neither the simulated nor the experimentally measured vibrational spectra of the OD band reports any appreciable shift. In Figure 6, we compare the amount of the peak shift ($\Delta\omega = \omega_{\text{osmolyte-water}} - \omega_{\text{water}}$) and the Δfwhm (= $\text{fwhm}_{\text{osmolyte-water}} - \text{fwhm}_{\text{water}}$, fwhm = full width at half-maximum) as obtained from the numerically simulated and experimental data.[31] The trend of the experimentally observed red shift of the OD band on addition of protecting osmolytes is well-reflected in the numerically simulated spectra. Nonetheless, even though the experimentally obtained $\Delta\omega$ correlates well with the one obtained from the numerical simulation in the case of the TMG, Δfwhm does not especially at higher concentration of TMG (Figure 6). In the case of sorbitol, the experimentally obtained Δfwhm correlates well with the one obtained from the numerical simulation, but $\Delta\omega$ does not do so well. However, urea's concentration-independent behavior is well-reflected in both the experimentally measured and numerically simulated ones for both the observables $\Delta\omega$ and Δfwhm. Considering the uncertainties in the vibrational solvatochromic charges determined by performing multivariate least-squares analyses of limited numbers of HDO−water clusters excluding osmolyte molecules, the present theoretical results in calculation of fwhm for IR spectra are found to be quite accurate.

Let us look into the origin of these peak shift behaviors of the OD vibrational bands on addition of the osmolytes. To examine how surrounding water and osmolyte molecules around an OD group affect the frequency of the OD stretch mode, the instantaneous OD frequency given in eq 1 is dissected into two terms that are one for water and the other for osmolyte contribution, that is, $\Delta\omega(\phi) = \Delta\omega^{\text{water}}(\phi) + \Delta\omega^{\text{osmolyte}}(\phi)$. The $\Delta\omega^{\text{water}}(\phi)$ and $\Delta\omega^{\text{osmolyte}}(\phi)$ were calculated using eq 1 with the consideration that water and osmolyte molecules are making either direct H-bonding or electrostatic interaction with the HDO molecule in the first hydration shell. The contributions from the osmolyte and water terms are separately plotted for all the three osmolyte solutions in Figure 7, where the x-axis represents the total frequency shift $\Delta\omega(\phi)$. In general, with the increase in the osmolyte concentration, the contribution of the water term ($\Delta\omega^{\text{water}}(\phi)$) in determining the frequency shift decreases, and accordingly the contribution of the osmolyte term increases ($\Delta\omega^{\text{osmolyte}}(\phi)$). But the overall concentration-dependent decreasing or increasing pattern depends on the type of the osmolyte molecule and osmolyte−osmolyte aggregation behavior. The magnitude of decrease of the water term is huge with the increasing concentration of TMG (especially in most populous frequency shift region of −200 to −300 cm^{-1}; Figure 2), while sorbitol causes just a moderate reduction in the amount of the water contribution term (blue arrow in Figure 7). Accordingly, the increase of the osmolyte contribution term (red arrow) is substantial in case of TMG, while sorbitol brings a moderate increase in the osmolyte contribution term with increasing concentrations of the osmolytes. Altogether, the decrease in the water term is more than compensated by the increase in the

DOI: 10.1021/acs.jpca.6b06305
J. Phys. Chem. A 2016, 120, 5874−5886

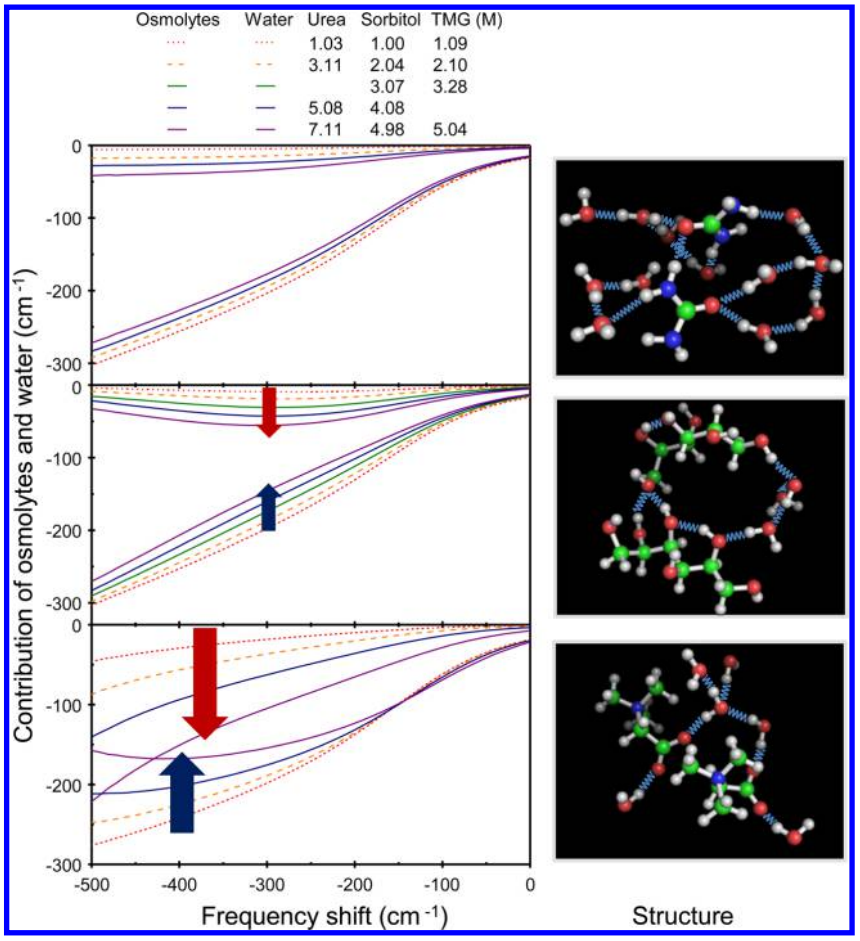

Figure 7. Separated contribution of the water and osmolyte terms in determining the OD frequency (x-axis) using eq 1 in the left column. The red (blue) colored arrow in the left column indicates the increasing (decreasing) contribution of the osmolyte (water) term as the concentration of osmolyte increases. TMG molecule exhibits dramatic change in each contribution term depending upon concentration. The water−osmolyte structure obtained from MD trajectory is plotted in the right column for urea, sorbitol, and TMG solutions. The blue wavy lines represent the interaction between osmolyte molecules, and surrounding water molecules.

osmolyte term and hence a net red shift effect of the OD frequency shift in the case of protecting osmolytes. In contrast, the addition of urea causes a minor decrease in the water term and similar minor increase in the osmolyte term with no net effect to be seen on the OD frequency shift. Such a concentration-dependent behavior of the protecting and independent behavior of the destabilizing osmolyte can be understood by looking into the local water H-bond structure at the molecular level as shown in the right side of Figure 7. Urea molecules, because of their unique size and H-bond forming capability,[29,35,74] seem to position themselves in a way to preserve water's tetrahedral H-bond network as much as possible. Sorbitol being a linear and flexible molecule with six available hydroxyl groups can form H bonds among themselves as well as to other molecules present in the vicinity. Such diversity in H-bonding capability compensates for the H-bonding partner, and hence the frequency shift term associated with water or osmolyte contribution (sorbitol) is moderate when compared to TMG at similar concentration. Note that TMG has a hydrophobic bulky trimethyl group at its one end, and the other end has a hydrophilic carboxylic group.

Similar to the way we separated the frequency shift into water and osmolyte terms, we also calculated the contributions of water and osmolyte molecules to the OD transition dipole moment separately (Figure 8). Although the transition dipole strength and transition frequency are mainly determined by the contribution associated with direct interaction of HDO with water and osmolyte molecules or both within its first hydration shell, the long-range interaction beyond the first shell also contributes to those vibrational properties. This long-range interaction is roughly estimated to be 20−40% of the total transition dipole moment depending upon the type and concentration of the osmolytes. In Figure 8, we present the z-component of the transition dipole moment of the water and the osmolyte separately (left side of Figure 8) as well as their sum (right side).

The magnitude of increase in the z-component of the transition dipole moment of the osmolyte term is more than the decrease in that of the water term with the increasing concentration of TMG. Looking closely into the concentration-dependent increase (decrease) of the z-component of the transition dipole moment of the osmolyte term (water term), it appears that the magnitude of the increase (decrease) is relatively larger in the frequency region of less than −250 cm^{-1} (center point in frequency shift distribution peak for TMG solutions in Figure 2) than the increase (decrease) in the frequency region of greater than −250 cm^{-1}. This net effect of concentration-dependent increase (especially in the frequency region of less than −250 cm^{-1}) in the magnitude of the $|\mu^{osmolyte+water}|$ for TMG, in combination with the $\Delta\omega(\phi)$

DOI: 10.1021/acs.jpca.6b06305
J. Phys. Chem. A 2016, 120, 5874−5886

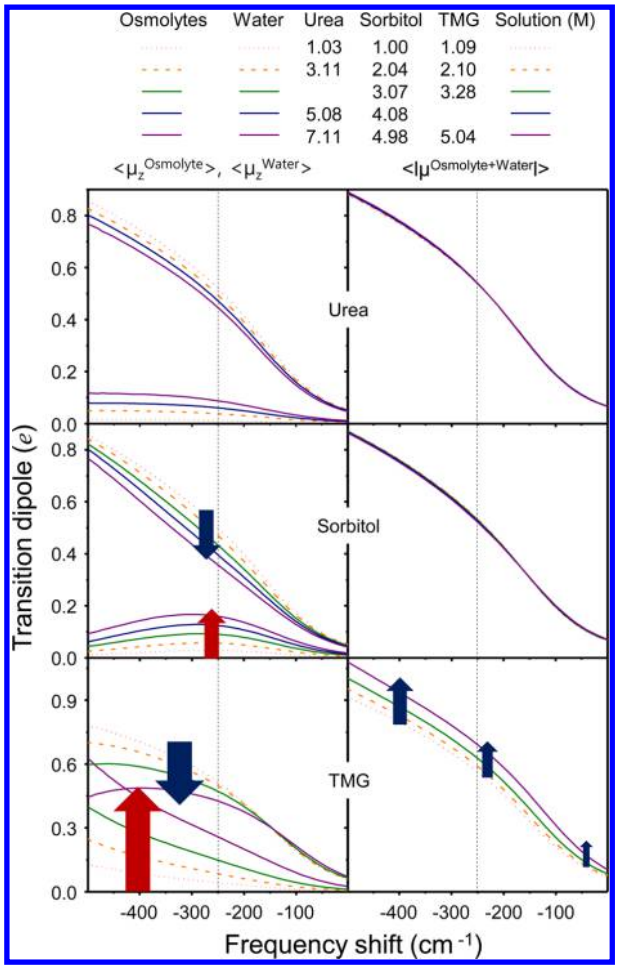

Figure 8. Separated contribution of the water and osmolyte terms in determining the OD transition dipole moment by using eq 2 in the left panel. It is the *z*-component of the transition dipole vector vs the frequency shift, which is plotted in the left column at various osmolyte concentrations. The absolute magnitudes of transition dipole vector (sum of water and osmolyte contribution terms) are plotted with respect to frequency shift at various concentrated solutions in the right column.

(Figure 7), causes a significant red shift of the OD band (Figure 5). In the case of sorbitol, the increase (decrease) in both the *z*-component of the transition dipole moment of osmolyte and $\Delta\omega^{\text{osmolyte}}(\phi)$ (the *z*-component of the transition dipole moment of water and $\Delta\omega^{\text{water}}(\phi)$) is significant in the central region (-250 cm^{-1}) of the frequency shift distribution (Figure 2). This moderate net increase in the transition dipole moment and $\Delta\omega(\phi)$ makes the OD peak to shift red with the increasing concentration of sorbitol (Figure 5). In contrast to the protecting osmolytes, both the transition dipole moment (Figures 4 and 8) and $\Delta\omega(\phi)$ (Figures 2 and 4) remain almost independent of the urea concentration, and hence a negligible shift in the OD frequency of HDO on addition of urea is observed.

Last but not least, we address the contribution of polarization effect on the vibrational transition dipole in the description of the line shape of the IR absorption spectrum in binary osmolyte−water solution. The importance of the inclusion of the polarization effect of water in calculating IR spectrum of OD in highly concentrated aqueous salt solution has been shown previously in our recent work.[34] We found that the *x*-component of the transition dipole vector contributes significantly to the numerical description of the OD line shape of the IR absorption spectrum at high concentration of salt solutions but not in pure liquid water. In Figure 9 we plot

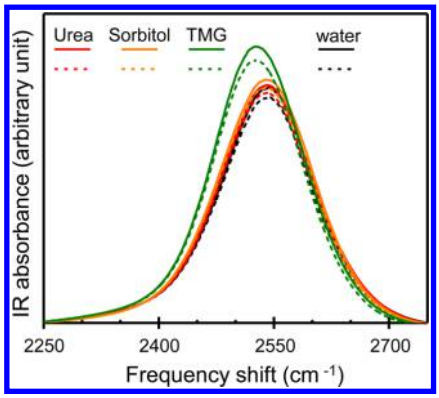

Figure 9. Numerically simulated IR spectra of urea (7.11 M), sorbitol (4.98 M), and TMG (5.04 M) solutions are plotted with (solid lines) and without (broken lines) taking into consideration the *x*-component of the transition dipole vector.

the calculated IR absorption spectra with (solid lines) and without (dotted lines) the contributions of the *x*-transition dipole components. There is a notable difference in the IR spectrum after the inclusion of the *x*-component of the OD transition dipole moment, especially in highly concentrated osmolyte solutions. Thus, we believe that the polarization effect on the OD transition dipole moment should be considered to quantitatively describe the IR absorption spectrum of the OD stretch mode in the presence of high concentrations of solutes.

There is a possibility that the OD IR absorption spectrum of the HDO might have additional contributions from either the acidic protons, that is, ND of urea or OD of sorbitol (sorbitol has six OH groups that can be exchanged with deuterium present in the solution). Recently, Skinner and co-workers analyzed experimental IR band shape using two fitting functions with Lorentzian line shape within OD (ND) stretch mode frequency region and suggested that the ND peak in urea is not discernibly contributed to IR spectrum within OD frequency region of HDO depending upon concentration.[35] In the case of sorbitol, we simulated the OD IR absorption spectrum of both HDO and sorbitol separately (data shown in the Supporting Information). In both cases, we find that the OD peak frequency undergoes red shift with the increasing concentration of the sorbitol.

IV.B. Translational and Orientational Dynamics of Water in Osmolyte Solutions. The translational mobility of a water molecule is described in terms of the time evolution of the mean-squared center of mass displacement. With the Einstein expression, one can obtain the self-diffusion coefficient of water (D_w) as follows

$$6Dt = \lim_{t\to\infty} \langle |r_i(t) - r_i(0)|^2 \rangle \tag{5}$$

where the angular bracket denotes a statistical average. The calculated D_w values along with the translational time of water are listed in Table 2. For pure water, D_w was estimated to be 3.7 $\times$ 10^{-5} cm^2 s^{-1}, which is slightly larger than the experimental value of 2.4 $\times$ 10^{-5} cm^2 s^{-1}. This discrepancy could be due to the inaccuracy of MD force field parameters for water. The D_w value decreases linearly with the increasing concentration of

DOI: 10.1021/acs.jpca.6b06305
J. Phys. Chem. A 2016, 120, 5874−5886

Table 2. Rotational Time Constant Obtained from the Mono-Exponential Fitting of Both the Numerically Simulated and the Experimentally Measured Rotational Anisotropy Decays of Three Different Osmolytes at Various Concentrations

numerically simulated				experimentally measured	
concentration (M)	τ_{rot} (ps)	water self-diffusion coefficient,[a] D_w (1×10^{-5} cm^2 s^{-1})	translatioanl time,[a] t_w (ps)	concentration (M)	τ_{rot} (ps)
		urea			
1.03	1.31	3.72	4.0	2.0	2.5 ± 0.6
3.11	1.36	3.33	4.5	4.0	2.5 ± 0.7
5.08	1.42	2.99	5.0	6.0	2.3 ± 1.1
7.11	1.53	2.53	5.9	8.0	2.2 ± 1.2
		sorbitol			
1.00	1.71	3.02	4.9	1.0	2.6 ± 0.05
2.04	2.45	2.06	7.3	2.0	4.7 ± 0.21
3.07	3.92	1.35	11.1	3.0	5.8 ± 1.02
4.08	6.27	0.76	19.6	4.0	6.9 ± 0.51
4.98	9.42	0.45	33.2	5.0	10.6 ± 0.82
		TMG			
1.09	1.68	3.09	4.8	1.0	2.4 ± 0.03
2.10	2.29	2.45	6.1	2.0	3.2 ± 0.07
3.28	3.74	1.54	9.7	3.0	3.9 ± 0.14
5.04	9.13	0.62	24.2	4.0	5.9 ± 0.22
				5.0	9.7 ± 0.84

[a]The calculated water self-diffusion coefficient (D_w) and its translational time (t_w) as a function of osmolytes concentration.

sorbitol and TMG in solutions. Interestingly, our observation that the decreasing rate of D_w value as sorbitol increases corroborates well with the experimental result on water diffusion coefficient in similar carbohydrate solutions.[75] However, in the case of urea, a marginal decrease in D_w is understandable because of the ability of urea to accommodate itself in water's tetrahedral network structure without causing any significant destruction of water H-bonding network. With eq 5, we calculated the characteristic translational time of water (t_w), which is the time required by a water molecule to cover a distance equivalent to its own diameter, ~3 Å. The results for t_w are listed in Table 2. On average, a single water molecule travels a distance of 3 Å in 4 ps in the pure water, whereas it takes ~33, 24, and 6 ps to cover the same distance in the 4.98 M solution of sorbitol, 5.04 M solution of TMG, and 7.11 M solution of urea, respectively. This clearly shows that water's translation motion is significantly slowed by the presence of osmolytes, sorbitol, and TMG.

The orientation mobility of a water molecule depends on both the rigidity of the H-bond network and the availability of the H-bonding partner.[76−78] To compare with the experimentally measured rotational relaxation, we calculated anisotropy decay $r(t)$ using the rotational time correlation function $C_{rot}(t)$

$$r(t) = \frac{2}{5}C_{rot}(t) = \frac{2}{5}\left\langle \frac{3[\hat{\mu}(0)\cdot\hat{\mu}(t)]^2 - 1}{2} \right\rangle \quad (6)$$

Here, $\hat{\boldsymbol{\mu}}$ (t) is the unit vector of the time-varying transition dipole moment of OD stretch mode. The calculated rotational anisotropy decays are plotted along with the experimentally measured ones in Figure 10. The agreement between them is found to be excellent, except that the experimental anisotropy decays are devoid of the initial ultrafast decay component (<200 fs) associated with librational motion of the water molecules.[79] The experimental data were fitted from 0.4 ps to avoid the cross-correlation of the pump and probe pulses as well as the ultrafast fast librational motion. Sorbitol has six hydroxyl (OH) groups and hence, the hydroxyl groups of

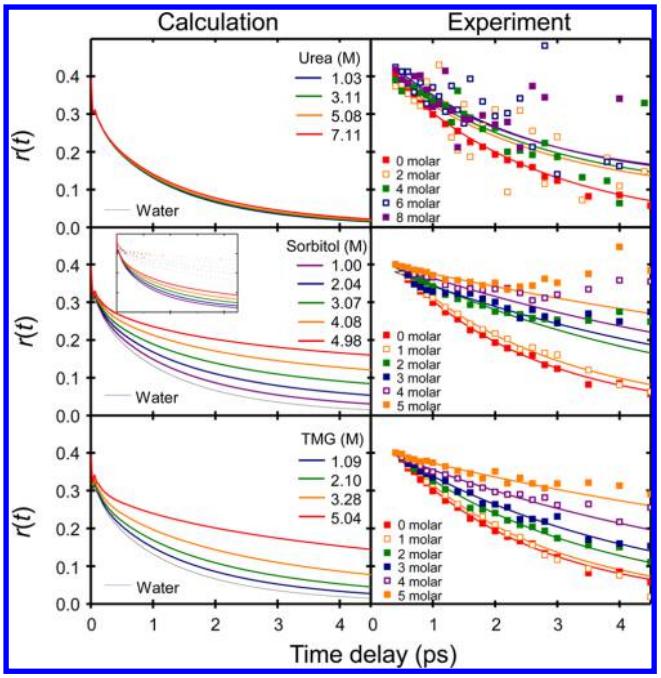

Figure 10. Numerically simulated rotational anisotropy decay (left column) of the OD stretch mode of HDO in osmolyte solutions are directly compared with the experimentally measured ones (right column; the symbols represent the raw data, and the solid line are fits to a monoexponential decaying function). The solid lines in the inset figure represent the rotational anisotropy decay of HDO without considering the contribution of the sorbitol's OD group, while the dashed lines indicate the anisotropy decay of the OD group of sorbitol only.

sorbitol has a tendency to be exchanged with deuterium present in the isotopically diluted (5% HDO) solution. Assuming the exchange rate of deuterium either with water or sorbitol to be similar, the population of deuterium substituted sorbitol was also estimated and included in the calculation of $r(t)$. The anisotropy decay of the OD of HDO and that of sorbitol are

DOI: 10.1021/acs.jpca.6b06305
J. Phys. Chem. A 2016, 120, 5874−5886

shown in the inset of Figure 10. As expected, the OD of sorbitol rotationally relaxes very slowly in comparison to that of HDO. In general, addition of osmolytes retards the rotational relaxation, but the extent of retardation depends on the type of the osmolyte.[29,31,32]

In pure water, complete reorientation relaxation involves both breaking and reforming of H bonds via water molecules in a special H-bonded configuration in which the hydroxyl group forms a weak, bifurcated H bond to two other water molecules. Any process that limits the accessibility of the new H-bond acceptor during the H-bond exchange process will slow the rotational relaxation.[80] TMG with a bulky trimethyl group hinders the approach of a new H-bond partner in its vicinity due to the excluded volume effect, and hence the water reorientation time increases with increasing concentration of TMG.[31] Sorbitol with its flexible and multiple H-bond forming capability slows the water reorientation considerably too, as shown in Figure 10, which is due to its long-range interaction with water molecules beyond its first hydration shell. In contrast, urea shows a weak concentration-dependence of the rotational relaxation dynamics of the OD probe.[29,31,35] Even at very high concentration such as 8 M, the rotational relaxation is similar to that of bulk water, which is again consistent with the notion that urea molecules accommodate well in the tetrahedral network of water without causing significant perturbation to the local water H-bond network. To extract the rotational time constant (τ_{rot}), the numerically calculated anisotropy decays were fitted with $A \exp(-t/\tau_{rot}) + B$, where B is a constant offset (suggesting a very slowly relaxing component if not zero). The τ_{rot} are summarized in Table 2 along with the fitting data of the experimentally measured anisotropy decays.[31] Thus, determined τ_{rot} from the theoretical calculation is also plotted with respect to osmolyte concentration in parallel with the experimentally measured rotational relaxation time constants in Figure 6, and the agreement between the theoretical and the experimental results is excellent. However, in the case of urea, the experimentally measured rotational anisotropy exhibits an offset that is found to increase in magnitude with the increasing concentration of urea (Table 2). This offset was believed to originate from the presence of strongly immobilized water molecules near urea, which are unable to reorient in the experimental time window of the anisotropy decay.[29,31] The present theoretical simulation results however provide little evidence on the presence of such immobilized water with very slow rotational relaxation. Carr et al. in ref 35 performed MD simulation with both optimized potentials for liquid simulations TIP4P and Kirkwood-Buff force field SPC/E potentials for comparison. They showed that the latter force field works reasonably well when their frequency map is used, but the former force field overestimates the frequency blue shift of OD stretch and makes little slowdown in the anisotropy of OD mode as urea concentration increases. Therefore, a further investigation with various force fields for not just water but also osmolytes would still be needed.

V. SUMMARY

Combining the distributed solvatochromic charge model developed by us with the MD simulation method, we were able to describe the time-varying vibrational frequency shifts, transition dipole moments, and rotational relaxations of the OD stretch mode of HDO in protecting and destabilizing osmolyte solutions at various concentrations. Both the x- and z-components of the OD transition dipole vector were taken into account by employing the charge response kernel term. The ensemble average OD stretch frequency undergoes a red shift, and the magnitude of the OD transition dipole moment increases with increasing concentration of the protecting osmolyte. In contrast, urea does not show any appreciable concentration-dependent change either in the OD stretch frequency distribution or in the transition dipole moment distribution. Separately considering the contributions from neighboring osmolyte and water molecules to the OD frequency shift and the OD transition dipole moment, we were able to find that the concentration-dependent red shift of the OD peak frequency in TMG and sorbitol was mostly due to the contribution from the osmolyte term. In contrast, the case of urea is special because the contribution originating from the osmolyte term roughly counterbalances the contribution originating from the water term, which results in no appreciable net effects on the OD frequency and the OD transition dipole moment. Hence, the OD stretch IR spectrum of HDO in urea solution does not depend on urea concentration. Not only the OD stretch frequencies but also the anisotropy decays of the OD band in all three osmolytes at various concentrations were calculated. All these computational simulation results being in excellent agreement with the experimentally measured results suggest that there are certain changes in the local water H-bond network and in the global morphological features, but the magnitude and the spatial extent of the osmolyte-induced perturbation vary greatly. Protecting osmolytes show strong concentration-dependent behaviors (vibrational frequencies and rotational relaxations), while denaturant urea does not. These quantitative agreements between the computational (IR spectrum and anisotropy decay of OD probe) and the experiment results clearly show the validity of the present theoretical approach in simulating and interpreting the linear (and possibly nonlinear) vibrational spectroscopic properties of the OD stretch mode in various osmolyte solutions. Currently, water structure and dynamics at the surfaces of lipid bilayers that have been revealed by either IR pump−probe or IR−vis sum-frequency-generation spectroscopy are under investigation with the approach used here in this paper.

■ ASSOCIATED CONTENT

Supporting Information

The Supporting Information is available free of charge on the ACS Publications website at DOI: 10.1021/acs.jpca.6b06305.

Numerically simulated OD stretch spectrum of sorbitol and HDO at different concentrations of sorbitol (PDF)

■ AUTHOR INFORMATION

Corresponding Author

*E-mail: mcho@korea.ac.kr. Phone: +82-2-3290-3133.

Author Contributions

‖These two authors contributed equally to this work.

Notes

The authors declare no competing financial interest.

■ ACKNOWLEDGMENTS

This work was supported by IBS-R023-D1. J.H.C. is thankful for financial supports from Korea University Grant and NRF fund (Grant Nos. 2014063491 and 2014044452).

DOI: 10.1021/acs.jpca.6b06305
J. Phys. Chem. A 2016, 120, 5874−5886

REFERENCES

(1) Yancey, P. H. Water Stress, Osmolytes and Proteins. *Am. Zool.* **2001**, *41*, 699−709.
(2) Brocker, C.; Thompson, D. C.; Vasiliou, V. The Role of Hyperosmotic Stress in Inflammation and Disease. *Biomol. Concepts* **2012**, *3*, 345−364.
(3) Jackson-Atogi, R.; Sinha, P. K.; Rösgen, J. Distinctive Solvation Patterns Make Renal Osmolytes Diverse. *Biophys. J.* **2013**, *105*, 2166−2174.
(4) Bakulin, A. A.; Liang, C.; la Cour Jansen, T.; Wiersma, D. A.; Bakker, H. J.; Pshenichnikov, M. S. Hydrophobic Solvation: A 2D IR Spectroscopic Inquest. *Acc. Chem. Res.* **2009**, *42*, 1229−1238.
(5) Stirnemann, G.; Sterpone, F.; Laage, D. Dynamics of Water in Concentrated Solutions of Amphiphiles: Key Roles of Local Structure and Aggregation. *J. Phys. Chem. B* **2011**, *115*, 3254−3262.
(6) Homsi Brandeburgo, W.; van der Post, S. T.; Meijer, E. J.; Ensing, B. On the Slowdown Mechanism of Water Dynamics around Small Amphiphiles. *Phys. Chem. Chem. Phys.* **2015**, *17*, 24968−24977.
(7) Kraemer, D.; Cowan, M. L.; Paarmann, A.; Huse, N.; Nibbering, E. T. J.; Elsaesser, T.; Miller, R. J. D. Temperature Dependence of the Two-Dimensional Infrared Spectrum of Liquid H_2O. *Proc. Natl. Acad. Sci. U. S. A.* **2008**, *105*, 437−442.
(8) Cowan, M. L.; Bruner, B. D.; Huse, N.; Dwyer, J. R.; Chugh, B.; Nibbering, E. T. J.; Elsaesser, T.; Miller, R. J. D. Ultrafast Memory Loss and Energy Redistribution in the Hydrogen Bond Network of Liquid H_2O. *Nature* **2005**, *434*, 199−202.
(9) Lawrence, C. P.; Skinner, J. L. Vibrational Spectroscopy of HOD in Liquid D_2O. II. Infrared Line Shapes and Vibrational Stokes Shift. *J. Chem. Phys.* **2002**, *117*, 8847−8854.
(10) Lawrence, C. P.; Skinner, J. L. Vibrational Spectroscopy of HOD in Liquid D_2O. III. Spectral Diffusion, and Hydrogen-Bonding and Rotational Dynamics. *J. Chem. Phys.* **2003**, *118*, 264−272.
(11) Mikenda, W. Stretching Frequency Versus Bond Distance Correlation of OD(H)···Y (Y N, O, S, Se, Cl, Br, I) Hydrogen Bonds in Solid Hydrates. *J. Mol. Struct.* **1986**, *147*, 1−15.
(12) Eaves, J. D.; Loparo, J. J.; Fecko, C. J.; Roberts, S. T.; Tokmakoff, A.; Geissler, P. L. Hydrogen Bonds in Liquid Water Are Broken Only Fleetingly. *Proc. Natl. Acad. Sci. U. S. A.* **2005**, *102*, 13019−13022.
(13) Loparo, J. J.; Roberts, S. T.; Tokmakoff, A. Multidimensional Infrared Spectroscopy of Water. II. Hydrogen Bond Switching Dynamics. *J. Chem. Phys.* **2006**, *125*, 194522.
(14) Loparo, J. J.; Roberts, S. T.; Tokmakoff, A. Multidimensional Infrared Spectroscopy of Water. I. Vibrational Dynamics in Two-Dimensional IR Line Shapes. *J. Chem. Phys.* **2006**, *125*, 194521.
(15) Asbury, J. B.; Steinel, T.; Kwak, K.; Corcelli, S. A.; Lawrence, C. P.; Skinner, J. L.; Fayer, M. D. Dynamics of Water Probed with Vibrational Echo Correlation Spectroscopy. *J. Chem. Phys.* **2004**, *121*, 12431−12446.
(16) Asbury, J. B.; Steinel, T.; Stromberg, C.; Corcelli, S. A.; Lawrence, C. P.; Skinner, J. L.; Fayer, M. D. Water Dynamics: Vibrational Echo Correlation Spectroscopy and Comparison to Molecular Dynamics Simulations. *J. Phys. Chem. A* **2004**, *108*, 1107−1119.
(17) Piatkowski, L.; de Heij, J.; Bakker, H. J. Probing the Distribution of Water Molecules Hydrating Lipid Membranes with Ultrafast Förster Vibrational Energy Transfer. *J. Phys. Chem. B* **2013**, *117*, 1367−1377.
(18) Bakker, H. J.; Skinner, J. L. Vibrational Spectroscopy as a Probe of Structure and Dynamics in Liquid Water. *Chem. Rev.* **2010**, *110*, 1498−1517.
(19) Deàk, J. C.; Rhea, S. T.; Iwaki, L. K.; Dlott, D. D. Vibrational Energy Relaxation and Spectral Diffusion in Water and Deuterated Water. *J. Phys. Chem. A* **2000**, *104*, 4866−4875.
(20) Smith, J. D.; Cappa, C. D.; Wilson, K. R.; Cohen, R. C.; Geissler, P. L.; Saykally, R. J. Unified Description of Temperature-Dependent Hydrogen-Bond Rearrangements in Liquid Water. *Proc. Natl. Acad. Sci. U. S. A.* **2005**, *102*, 14171−14174.
(21) Laenen, R.; Rauscher, C.; Laubereau, A. Dynamics of Local Substructures in Water Observed by Ultrafast Infrared Hole Burning. *Phys. Rev. Lett.* **1998**, *80*, 2622−2625.
(22) Rezus, Y. L. A.; Bakker, H. J. On the Orientational Relaxation of HDO in Liquid Water. *J. Chem. Phys.* **2005**, *123*, 114502.
(23) Fayer, M. D.; Moilanen, D. E.; Wong, D.; Rosenfeld, D. E.; Fenn, E. E.; Park, S. Water Dynamics in Salt Solutions Studied with Ultrafast Two-Dimensional Infrared (2D IR) Vibrational Echo Spectroscopy. *Acc. Chem. Res.* **2009**, *42*, 1210−1219.
(24) Park, S.; Fayer, M. D. Hydrogen Bond Dynamics in Aqueous NaBr Solutions. *Proc. Natl. Acad. Sci. U. S. A.* **2007**, *104*, 16731−16738.
(25) Omta, A. W.; Kropman, M. F.; Woutersen, S.; Bakker, H. J. Negligible Effect of Ions on the Hydrogen-Bond Structure in Liquid Water. *Science* **2003**, *301*, 347−349.
(26) Giammanco, C. H.; Wong, D. B.; Fayer, M. D. Water Dynamics in Divalent and Monovalent Concentrated Salt Solutions. *J. Phys. Chem. B* **2012**, *116*, 13781−13792.
(27) Wong, D. B.; Sokolowsky, K. P.; El-Barghouthi, M. I.; Fenn, E. E.; Giammanco, C. H.; Sturlaugson, A. L.; Fayer, M. D. Water Dynamics in Water/DMSO Binary Mixtures. *J. Phys. Chem. B* **2012**, *116*, 5479−5490.
(28) Fenn, E. E.; Moilanen, D. E.; Levinger, N. E.; Fayer, M. D. Water Dynamics and Interactions in Water−Polyether Binary Mixtures. *J. Am. Chem. Soc.* **2009**, *131*, 5530−5539.
(29) Rezus, Y. L. A.; Bakker, H. J. Effect of Urea on the Structural Dynamics of Water. *Proc. Natl. Acad. Sci. U. S. A.* **2006**, *103*, 18417−18420.
(30) Rezus, Y. L. A.; Bakker, H. J. Destabilization of the Hydrogen-Bond Structure of Water by the Osmolyte Trimethylamine N-Oxide. *J. Phys. Chem. B* **2009**, *113*, 4038−4044.
(31) Verma, P. K.; Lee, H.; Park, J.-Y.; Lim, J.-H.; Maj, M.; Choi, J.-H.; Kwak, K.-W.; Cho, M. Modulation of the Hydrogen Bonding Structure of Water by Renal Osmolytes. *J. Phys. Chem. Lett.* **2015**, *6*, 2773−2779.
(32) Groot, C. C.; Bakker, H. J. A Femtosecond Mid-Infrared Study of the Dynamics of Water in Aqueous Sugar Solutions. *Phys. Chem. Chem. Phys.* **2015**, *17*, 8449−8458.
(33) Lee, H.; Choi, J.-H.; Verma, P. K.; Cho, M. Spectral Graph Analyses of Water Hydrogen-Bonding Network and Osmolyte Aggregate Structures in Osmolyte−Water Solutions. *J. Phys. Chem. B* **2015**, *119*, 14402−14412.
(34) Choi, J.-H.; Kim, H.; Kim, S.; Lim, S.; Chon, B.; Cho, M. Ion Aggregation in High Salt Solutions. III. Computational Vibrational Spectroscopy of HDO in Aqueous Salt Solutions. *J. Chem. Phys.* **2015**, *142*, 204102.
(35) Carr, J. K.; Buchanan, L. E.; Schmidt, J. R.; Zanni, M. T.; Skinner, J. L. Structure and Dynamics of Urea/Water Mixtures Investigated by Vibrational Spectroscopy and Molecular Dynamics Simulation. *J. Phys. Chem. B* **2013**, *117*, 13291−13300.
(36) Cho, M. Vibrational Solvatochromism and Electrochromism: Coarse-Grained Models and Their Relationships. *J. Chem. Phys.* **2009**, *130*, 094505.
(37) Choi, J.-H.; Hahn, S.; Cho, M. Amide I IR, VCD, and 2D IR Spectra of Isotope-Labeled Alpha-Helix in Liquid Water: Numerical Simulation Studies. *Int. J. Quantum Chem.* **2005**, *104*, 616−634.
(38) Choi, J.-H.; Hahn, S.; Cho, M. Vibrational Spectroscopic Characteristics of Secondary Structure Polypeptides in Liquid Water: Constrained MD Simulation Studies. *Biopolymers* **2006**, *83*, 519−536.
(39) Choi, J.-H.; Lee, H.; Lee, K.-K.; Hahn, S.; Cho, M. Computational Spectroscopy of Ubiquitin: Comparison between Theory and Experiments. *J. Chem. Phys.* **2007**, *126*, 045102.
(40) Jeon, J.; Yang, S.; Choi, J.-H.; Cho, M. Computational Vibrational Spectroscopy of Peptides and Proteins in One and Two Dimensions. *Acc. Chem. Res.* **2009**, *42*, 1280−1289.
(41) Choi, J.-H.; Oh, K.-I.; Lee, H.; Lee, C.; Cho, M. Nitrile and Thiocyanate IR Probes: Quantum Chemistry Caculation Studies and Multivariate Least-Square Fitting Analysis. *J. Chem. Phys.* **2008**, *128*, 134506.

DOI: 10.1021/acs.jpca.6b06305
J. Phys. Chem. A 2016, 120, 5874−5886

(42) Oh, K.-I.; Choi, J.-H.; Lee, J.-H.; Han, J.-B.; Lee, H.; Cho, M. Nitrile and Thiocyanate IR Probes: Molecular Dynamics Simulation Studies. *J. Chem. Phys.* **2008**, *128*, 154504.
(43) Choi, J.-H.; Oh, K.-I.; Cho, M. Azido-Derivatized Compounds as IR Probes of Local Electrostatic Environment: Theoretical Studies. *J. Chem. Phys.* **2008**, *129*, 174512.
(44) Choi, J.-H.; Kwak, K.-W.; Cho, M. Computational Infrared and Two-Dimensional Infrared Photon Echo Spectroscopy of Both Wild-Type and Double Mutant Myoglobin-CO Proteins. *J. Phys. Chem. B* **2013**, *117*, 15462−15478.
(45) Loparo, J. J.; Roberts, S. T.; Nicodemus, R. A.; Tokmakoff, A. Variation of the Transition Dipole Moment across the OH Stretching Band of Water. *Chem. Phys.* **2007**, *341*, 218−229.
(46) Auer, B. M.; Skinner, J. L. Dynamical Effects in Line Shapes for Coupled Chromophores: Time-Averaging Approximation. *J. Chem. Phys.* **2007**, *127*, 104105.
(47) Auer, B. M.; Skinner, J. L. IR and Raman Spectra of Liquid Water: Theory and Interpretation. *J. Chem. Phys.* **2008**, *128*, 224511.
(48) Choi, J.-H.; Cho, M. Computational IR Spectroscopy of Water: OH Stretch Frequencies, Transition Dipoles, and Intermolecular Vibrational Coupling Constants. *J. Chem. Phys.* **2013**, *138*, 174108.
(49) Schmidt, J. R.; Corcelli, S. A.; Skinner, J. L. Pronounced Non-Condon Effects in the Ultrafast Infrared Spectroscopy of Water. *J. Chem. Phys.* **2005**, *123*, 044513.
(50) Auer, B.; Kumar, R.; Schmidt, J. R.; Skinner, J. L. Hydrogen Bonding and Raman, IR, and 2D-IR Spectroscopy of Dilute HOD in Liquid D_2O. *Proc. Natl. Acad. Sci. U. S. A.* **2007**, *104*, 14215−14220.
(51) Hayashi, T.; la Cour Jansen, T.; Zhuang, W.; Mukamel, S. Collective Solvent Coordinates for the Infrared Spectrum of HOD in D_2O Based on an Ab Initio Electrostatic Map. *J. Phys. Chem. A* **2005**, *109*, 64−82.
(52) Corcelli, S. A.; Lawrence, C. P.; Skinner, J. L. Combined Electronic Structure/Molecular Dynamics Approach for Ultrafast Infrared Spectroscopy of Dilute HOD in Liquid H_2O and D_2O. *J. Chem. Phys.* **2004**, *120*, 8107−8117.
(53) Corcelli, S. A.; Skinner, J. L. Infrared and Raman Line Shapes of Dilute HOD in Liquid H_2O and D_2O from 10 to 90 °C. *J. Phys. Chem. A* **2005**, *109*, 6154−6165.
(54) Lin, Y.-S.; Auer, B. M.; Skinner, J. L. Water Structure, Dynamics, and Vibrational Spectroscopy in Sodium Bromide Solutions. *J. Chem. Phys.* **2009**, *131*, 144511.
(55) Breneman, C. M.; Wiberg, K. B. Determining Atom-Centered Monopoles from Molecular Electrostatic Potentials. The Need for High Sampling Density in Formamide Conformational Analysis. *J. Comput. Chem.* **1990**, *11*, 361−373.
(56) Frisch, M. J.; Trucks, G. W.; Schlegel, H. B.; Scuseria, G. E.; Robb, M. A.; Cheeseman, J. R.; Scalmani, G.; Barone, V.; Mennucci, B.; Petersson, G. A., et al. *Gaussian 09, Revision D.01;* Gaussian, Inc: Wallingford, CT, 2009.
(57) Wang, J.; Wolf, R. M.; Caldwell, J. W.; Kollman, P. A.; Case, D. A. Development and Testing of a General Amber Force Field. *J. Comput. Chem.* **2004**, *25*, 1157−1174.
(58) Cornell, W. D.; Cieplak, P.; Bayly, C. I.; Kollmann, P. A. Application of Resp Charges to Calculate Conformational Energies, Hydrogen Bond Energies, and Free Energies of Solvation. *J. Am. Chem. Soc.* **1993**, *115*, 9620−9631.
(59) Case, D. A.; Darden, T. A.; Cheatham, T. E., III; Simmerling, C. L.; Wang, J.; Duke, R. E.; Luo, R.; Walker, R. C.; Zhang, W.; Merz, K. M., *Amber 11;* University of California: San Francisco, CA, 2010.
(60) Darden, T.; York, D.; Pedersen, L. Particle Mesh Ewald - an N.Log(N) Method for Ewald Sums in Large Systems. *J. Chem. Phys.* **1993**, *98*, 10089−10092.
(61) Choi, J.-H.; Cho, M. Ion Aggregation in High Salt Solutions. IV. Graph-Theoretical Analyses of Ion Aggregate Structure and Water Hydrogen Bonding Network. *J. Chem. Phys.* **2015**, *143*, 104110.
(62) Biggs, N. *Algebraic Graph Theory;* Cambridge University Press: Cambridge, U.K, 1974.
(63) Strang, G. V. *Linear Algebra and Its Applications;* Harcourt Brace Jovanovich: San Diego, CA, 1988.
(64) Bako, I.; Bencsura, A.; Hermannson, K.; Balint, S.; Grosz, T.; Chihaia, V.; Olah, J. Hydrogen Bond Network Topology in Liquid Water and Methanol: A Graph Theory Approach. *Phys. Chem. Chem. Phys.* **2013**, *15*, 15163−15171.
(65) Batista da Silva, J. A.; Moreira, F. G. B.; Leite dos Santos, V. M.; Longo, R. L. On the Hydrogen Bond Networks in the Water-Methanol Mixtures: Topology, Percolation and Small-World. *Phys. Chem. Chem. Phys.* **2011**, *13*, 6452−6461.
(66) Kuharski, R. A.; Rossky, P. J. Molecular Dynamics Study of Solvation in Urea Water Solution. *J. Am. Chem. Soc.* **1984**, *106*, 5786−5793.
(67) Kokubo, H.; Pettitt, B. M. Preferential Solvation in Urea Solutions at Different Concentrations: Properties from Simulation Studies. *J. Phys. Chem. B* **2007**, *111*, 5233−5242.
(68) Soper, A. K.; Castner, E. W., Jr; Luzar, A. Impact of Urea on Water Structure: A Clue to Its Properties as a Denaturant? *Biophys. Chem.* **2003**, *105*, 649−666.
(69) Sokolić, F.; Idrissi, A.; Perera, A. Concentrated Aqueous Urea Solutions: A Molecular Dynamics Study of Different Models. *J. Chem. Phys.* **2002**, *116*, 1636−1646.
(70) Sapir, L.; Harries, D. Linking Trehalose Self-Association with Binary Aqueous Solution Equation of State. *J. Phys. Chem. B* **2011**, *115*, 624−634.
(71) Mukamel, S. *Principles of Nonlinear Optical Spectroscopy;* Oxford University Press: Oxford, U.K, 1995.
(72) McQuarrie, D. A. *Statistical Mechanics;* Harper & Row: New York, 1976.
(73) Steinel, T.; Asbury, J. B.; Zheng, J.; Fayer, M. D. Watching Hydrogen Bonds Break: A Transient Absorption Study of Water. *J. Phys. Chem. A* **2004**, *108*, 10957−10964.
(74) Kallies, B. Coupling of Solvent and Solute Dynamics-Molecular Dynamics Simulations of Aqueous Urea Solutions with Different Intramolecular Potentials. *Phys. Chem. Chem. Phys.* **2002**, *4*, 86−95.
(75) Feeney, M.; Brown, C.; Tsai, A.; Neumann, D.; Debenedetti, P. G. Incoherent Quasi-Elastic Neutron Scattering from Fructose−Water Solutions. *J. Phys. Chem. B* **2001**, *105*, 7799−7804.
(76) Fecko, C. J.; Loparo, J. J.; Roberts, S. T.; Tokmakoff, A. Local Hydrogen Bonding Dynamics and Collective Reorganization in Water: Ultrafast Infrared Spectroscopy of HOD/D_2O. *J. Chem. Phys.* **2005**, *122*, 054506.
(77) Woutersen, S.; Bakker, H. J. Resonant Intermolecular Transfer of Vibrational Energy in Liquid Water. *Nature* **1999**, *402*, 507−509.
(78) Yeremenko, S.; Pshenichnikov, M. S.; Wiersma, D. A. Hydrogen-Bond Dynamics in Water Explored by Heterodyne-Detected Photon Echo. *Chem. Phys. Lett.* **2003**, *369*, 107−113.
(79) Lin, Y.-S.; Pieniazek, P. A.; Yang, M.; Skinner, J. L. On the Calculation of Rotational Anisotropy Decay, as Measured by Ultrafast Polarization-Resolved Vibrational Pump-Probe Experiments. *J. Chem. Phys.* **2010**, *132*, 174505.
(80) Laage, D.; Hynes, J. T. Reorientional Dynamics of Water Molecules in Anionic Hydration Shells. *Proc. Natl. Acad. Sci. U. S. A.* **2007**, *104*, 11167−11172.

DOI: 10.1021/acs.jpca.6b06305
J. Phys. Chem. A 2016, 120, 5874−5886